

Effect of oxygen configurations on the mechanical properties of graphene oxide

Cite as: J. Appl. Phys. **132**, 174302 (2022); <https://doi.org/10.1063/5.0113425>

Submitted: 23 July 2022 • Accepted: 06 October 2022 • Published Online: 01 November 2022

Published open access through an agreement with JISC Collections

 Mohammad Nasr Esfahani,  Sepeedeh Shahbeigi and  Masoud Jabbari



View Online



Export Citation



CrossMark

ARTICLES YOU MAY BE INTERESTED IN

[A theoretical examination of localized nanoscale induction by single domain magnetic particles](#)

Journal of Applied Physics **132**, 174304 (2022); <https://doi.org/10.1063/5.0102153>

[Nanoscale infrared imaging and spectroscopy of few-layer hexagonal boron nitride](#)

Journal of Applied Physics **132**, 174301 (2022); <https://doi.org/10.1063/5.0107821>

[Effect of Mg-doping and Fe-doping in lead zirconate titanate \(PZT\) thin films on electrical reliability](#)

Journal of Applied Physics **132**, 174101 (2022); <https://doi.org/10.1063/5.0101308>



APL Quantum

CALL FOR APPLICANTS

Seeking Editor-in-Chief

Effect of oxygen configurations on the mechanical properties of graphene oxide

Cite as: J. Appl. Phys. **132**, 174302 (2022); doi: [10.1063/5.0113425](https://doi.org/10.1063/5.0113425)

Submitted: 23 July 2022 · Accepted: 6 October 2022 ·

Published Online: 1 November 2022



Mohammad Nasr Esfahani,^{1,a)} Sepeedeh Shahbeigi,² and Masoud Jabbari³

AFFILIATIONS

¹School of Physics, Engineering and Technology, University of York, York YO10 5DD, United Kingdom

²WMG, University of Warwick, Coventry CV4 7AL, United Kingdom

³Department of Mechanical, Aerospace and Civil Engineering, University of Manchester, Manchester M13 9PL, United Kingdom

^{a)}Author to whom correspondence should be addressed: mohammad.nasresfahani@york.ac.uk

ABSTRACT

Understanding the mechanical properties of graphene oxide (GO) is the primary challenge for applications in materials engineering. The degree of oxidation and concentration of epoxide functional groups have been the main focus of previous mechanochemical studies. This work uses the reactive molecular dynamic simulations to reveal that the mechanical behavior of GO is strongly dependent on the epoxide configuration as well as its distribution. In this study, three main epoxide configurations—including top, bridge, and reside groups—decorate monolayer GO sheets with linear and random distributions. The distortion associated with epoxide groups creates diamond-like structures controlling the mechanical properties. Moreover, the orientation of those epoxide functional groups with applied loads has a dramatic impact on the mechanical response of GO. The effect of external electric fields on the mechanical properties of GO is another objective of this study. Findings exhibit that the electric field enhances the tensile toughness. This study demonstrates new aspects of GO as a functional material with potentials to control the mechanical properties through chemical compositions as well as external electric fields.

© 2022 Author(s). All article content, except where otherwise noted, is licensed under a Creative Commons Attribution (CC BY) license (<http://creativecommons.org/licenses/by/4.0/>). <https://doi.org/10.1063/5.0113425>

I. INTRODUCTION

Graphene-based materials have been considered promising structures with novel applications in various fields due to their unique physical properties. Graphene oxide (GO) is oxygen-functionalized graphene offering chemically modified graphene for nanoelectronics,¹ sensing,² and composite³ technologies. This leads to a broad range of efforts to study remarkable features of GO that are particularly different from pristine graphene sheets.⁴ Experimental observations and theoretical studies have indicated two main functional groups in GO containing a hydroxyl (–OH) and epoxide (–O–) bonding on the basal plane,^{2,4} changing the physical and chemical behavior of nanoplatelets. Mechanical properties are among those features that are greatly influenced by these functional groups.⁴

Several studies have measured the mechanical behavior of GO sheets.^{5–10} As a primary outcome, a lower elastic modulus and strength is determined compared to pristine graphene sheets, which has been addressed through carbon bonding transformation from strong sp^2 bonds to a weaker sp^3 bonding. While hydroxyl

and epoxide groups reduce the mechanical properties of GO compared to unfunctionalized carbon-based materials, a wide range of mechanical behavior has been reported so far for GO sheets depending on the sample details. For example, an elastic modulus from 6 to 42 GPa and an intrinsic strength in a range of 76–293 MPa have been measured for multi-layers of GO.⁷ This contrast enhances for monolayer GO sheets, where an elastic modulus of 250 GPa is reported with a standard deviation of 150 GPa.⁵

Theoretical approaches have been developed to understand experimental measurements, which include a range of molecular dynamics (MD) simulations^{11–17} and density functional theories (DFT)^{18–20} focusing on the influence of functional groups on the mechanical behavior of GO sheets. For instance, DFT calculations have demonstrated the impact of epoxide and hydroxyl concentration on the deformation and fracture strength of monolayer GO.¹⁸ Although epoxide groups can enhance the GO ductility,¹⁸ numerous studies have revealed a significant reduction of the mechanical strength through increasing the concentration of functional groups.^{15,18,20} These changes in the mechanical properties can be

enhanced for multi-layer GO sheets.¹⁴ There has been significant attention focusing on the effect of functional group density^{14,15,20} and the epoxide-to-hydroxyl ratio,^{16,18} where the ratio of sp^3 bonds to sp^2 bonding has been considered a critical criterion to predict the mechanical properties of GO sheets. The influence of the functional group configuration and its distribution on the mechanical behavior become an immediate challenge for the characterization of GO sheets.

Various experimental studies have identified oxide-rich regions in GO.^{21–23} Previous studies have modeled those regions with different epoxide configurations focusing mainly on the effect of functional group density and the epoxide-to-hydroxyl ratio,^{15,16,18,20} while the impact of atomic structures of epoxide functional groups on the mechanical behavior of GO remains to be addressed. This work uses MD simulations to study the effect of epoxide configurations on the mechanical properties of monolayer GO. The present study employs the reactive force field potential to model the interaction between oxygen and carbon atoms. First, the influence of epoxide structures on the tensile properties is studied for GO with various oxide distributions. Next, the influence of electric fields on such functional groups is investigated. In the remainder, the MD model will be presented, followed by a discussion on the epoxide configurations. Then, the tensile behavior of GO will be studied for various epoxide groups with linear and random distributions. Finally, this work will be concluded by discussing the electric field effect on the mechanical response of GO sheets.

II. SIMULATION MODEL

The atomic structure of GO is complicated regarding the type and distribution of functional groups remaining controversial among experimental observations and theoretical models.^{4,5,20} Most theoretical studies are based on the Lerf-Kilnowski model focusing on the functional group density.^{2,4,11,20} The oxygen atoms in the epoxide group can create bonds with carbon atoms in the form of bridge, top, and reside, as shown in Fig. 1. The bridge

structure has a bond length of 1.464 Å.^{19,24} When an oxygen atom is attached to carbon atoms, covalent bonds form between the oxygen atom and carbon atoms. This bonding form changes the carbon bond length in graphene from an initial 1.42 to 1.58 Å constituting a transformation of an in-plane sp^2 structure to a three-dimensional sp^3 structure. Therefore, the bridge group creates two sp^3 structures, while the top group yields one sp^3 carbon atom. In another form, oxygen atoms sit entirely in the sheet plane, substituting with a carbon atom with a reside configuration as shown in Fig. 1(c). In this structure, oxygen atoms create bonds with carbon atoms with uneven distances of 1.513, 1.510, and 1.5 Å.²⁴ Various experimental observations identified different oxygen bonding in GO.^{22,23} Those oxygen configurations in epoxide groups have been modeled previously though studying mainly the influence of functional group density,^{15,18,20} while the effect of oxygen bonding in diamond-like structures necessitates to be addressed through a set of benchmark studies. This study focuses on the impact of such different epoxide configurations on the mechanical behavior of monolayer GO using MD simulations.

This work performs MD simulations in a large-scale atomic/molecular massively parallel simulator (LAMMPS).²⁵ The bonded and nonbonded interactions were modeled using the reactive force field (ReaxFF) potential,²⁶ which can capture the bond dynamic between carbon and oxygen atoms by determining the bond order empirically from the interatomic distance. This potential is considered a connection between non-reactive MD and quantum chemistry. In the ReaxFF potential, the energy of the system, E_{sys} , is a summation of various partial energy contributions as

$$E_{sys} = E_{bond} + E_{over} + E_{under} + E_{val} + E_{tor} + E_{pen} + E_{conj} + E_{vdwalls} + E_{coulomb}, \quad (1)$$

where E_{bond} is the bond energy, E_{over} and E_{under} are the over-coordination and under-coordination energy, respectively, E_{val} is the valence angle energy, E_{tor} is the energy associated with a torsion angle term, E_{pen} is the penalty energy of over-/undercoordination in a central atom, E_{conj} is the energy of conjunction effects, $E_{vdWalls}$ is the nonbonded van der Waals interactions, and $E_{coulomb}$ is the nonbond associated with Coulomb energies. In this study, the parameter set for the ReaxFF potential for the oxidation of a hydrocarbon is used to model GO.²⁶

This study considers a graphene sheet size of $50 \times 20 \text{ Å}^2$ with a periodic boundary condition along x - and y -directions (Fig. 2). This periodic boundary condition along in-plan directions eliminates any edge and size effects. In contrast, a thickness of 30 Å is considered along the z -direction with a fixed boundary condition to replicate a monolayer GO sheet. Various epoxide functional groups were defined with different distributions to create monolayer GO, where the oxygen density remains the same for all GO sheets. Linear and random distributions are considered for epoxide functional groups. This work denotes linear distributions perpendicular and parallel to the tensile load as V-linear and H-linear, respectively. The random number generator is used to locate epoxide groups on GO sheets with the random distribution.^{18,27} All simulations start with relaxation at a temperature of 300 K and a pressure of 0 bar using an isothermal-isobaric (NPT) ensemble

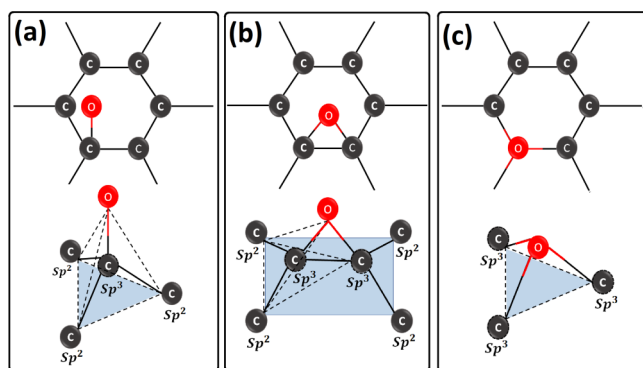


FIG. 1. Oxygen bonding with carbon atoms in GO having (a) top, (b) bridge, and (c) reside configurations creating diamond-like structures indicated with dashed lines. Oxygen and carbon atoms are indicated with red and gray colors, respectively. The blue shaded area indicates the in-plane of sp^2 hybridization of graphene sheets.

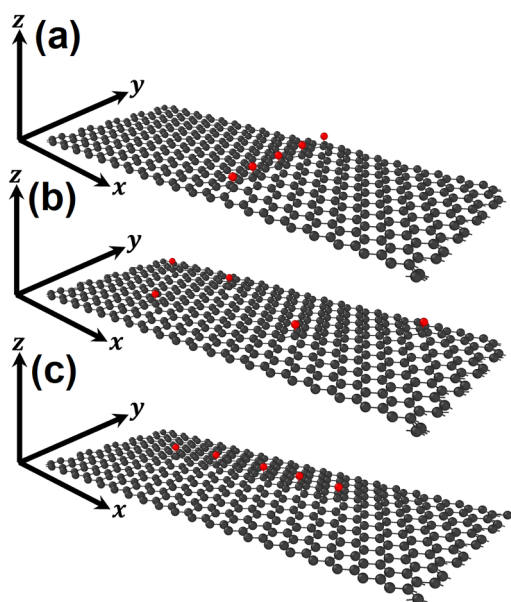


FIG. 2. Atomic structure of GO sheets with epoxide functional groups with (a) a linear distribution across the tensile load (V-linear), (b) a random distribution, and (c) a linear distribution along with the tensile load (H-linear). Oxygen and carbon atoms are indicated with red and gray colors, respectively.

with the Nosé–Hoover thermostat for 50 ps. Then, uniaxial tensile deformation is applied along the x -direction with a strain rate of $5 \times 10^{-4} \text{ ps}^{-1}$ at 300 K. All simulations are performed at a time step of 0.05 fs. The charge equilibrium process was carried out at every ten integration steps for all simulations.

The stress–strain graphs are used to measure the mechanical properties. Here, the elastic modulus is obtained as the slope of the linear elastic regime. The yield strength is estimated at the start of post-peaks, while the fracture strain is determined in the last post-peak before rupture. The fracture toughness is estimated by integrating the stress–strain curve. Simulations are initially validated by replicating previous works on the tensile tests of monolayer GO.^{13,18} Motivated by the application of electric fields in graphene-based devices,^{4,28–31} the impact of electric fields on the mechanical properties is another objective of the present study. Considering applications as electromechanical devices,^{28,29} the electric field is mainly applied perpendicular to GO sheets. In this respect, an electric field of 0.5 V/Å is applied perpendicular (z -direction) to GO sheets during the tensile deformation.

III. RESULTS AND DISCUSSION

In the first step, the impact of oxygen distribution is studied for various epoxide groups, including the top, bridge, and reside configurations, where those results are compared with pristine monolayer graphene. Table I lists the mechanical properties of pristine graphene and GO sheets with top, bridge, and reside epoxide groups in various distributions. Figure 3 exhibits the mechanical

TABLE I. The mechanical properties of pristine graphene and GO sheets with top, bridge, and reside epoxide groups in various distributions.

Epoxide config.	Elastic modulus (GPa)	Yield strength (GPa)	Fracture strain	Toughness (GJ/m ³)
Pristine graphene
V-linear distribution				
Top	506	48	0.119	3.0
Bridge	511	52	0.123	3.4
Reside	546	26	0.103	2.5
Random distribution				
Top	581	52	0.196	6.1
Bridge	531	61	0.175	5.9
Reside	486	34	0.124	3.8
H-linear distribution				
Top	549	59	0.225	8.2
Bridge	542	61	0.178	6.3
Reside	562	53	0.167	5.5

behavior of GO sheets with epoxide groups distributed in the V-linear form. The stress changes linearly until a yield point, where there is a drop in the stress. The stress then increases until the fracture occurs in the structures. This post-peak stress behavior is dramatically different for GO sheets. For example, the GO sheet with the top epoxide configuration exhibits a significant reduction in the post-peaks. The stress in GO with the bridge and reside epoxide structures drops slightly, followed by a considerable increase to the fracture point. In addition to the post-peak behavior, epoxide groups have different impacts on the mechanical response of GO sheets, which can be observed by comparing the yield strength, fracture strain, and toughness presented in Table I. The effect of the epoxide functional groups on the mechanical properties can be studied by analyzing the deformation response. Atomic configurations during the deformation at the yield and post-peaks indicated in the stress–strain graph [Fig. 3(a)] are shown in Figs. 3(b)–3(d). Starting from the top configuration, the C–C bonds between the epoxide and sp^2 break at the yield point [T1, Fig. 3(b)], while crack propagation is observed upon further loading through cleavage of sp^2 bonds [T2, Fig. 3(b)]. Although a similar bond break between sp^3 and sp^2 carbons is observed at the yield point of the bridge epoxide [B1, Fig. 3(c)], the GO sheet reaches a brittle fracture through breaking all epoxide bonds without any crack propagation [B2, Fig. 3(b)]. A deformation response in the reside epoxide group is found to be similar to the bridge configuration with a C–O bond break followed by a brittle fracture [Fig. 3(d)]. The strength of C–C bonds between epoxide and sp^2 constitutes the yielding in the top and bridge configurations, while the C–O bonds control the yield strength of the reside epoxide group.

Now, it is time to study the effect of epoxide groups with a random distribution. Figure 4 exhibits the mechanical properties of GO sheets with randomly distributed epoxide functional groups.

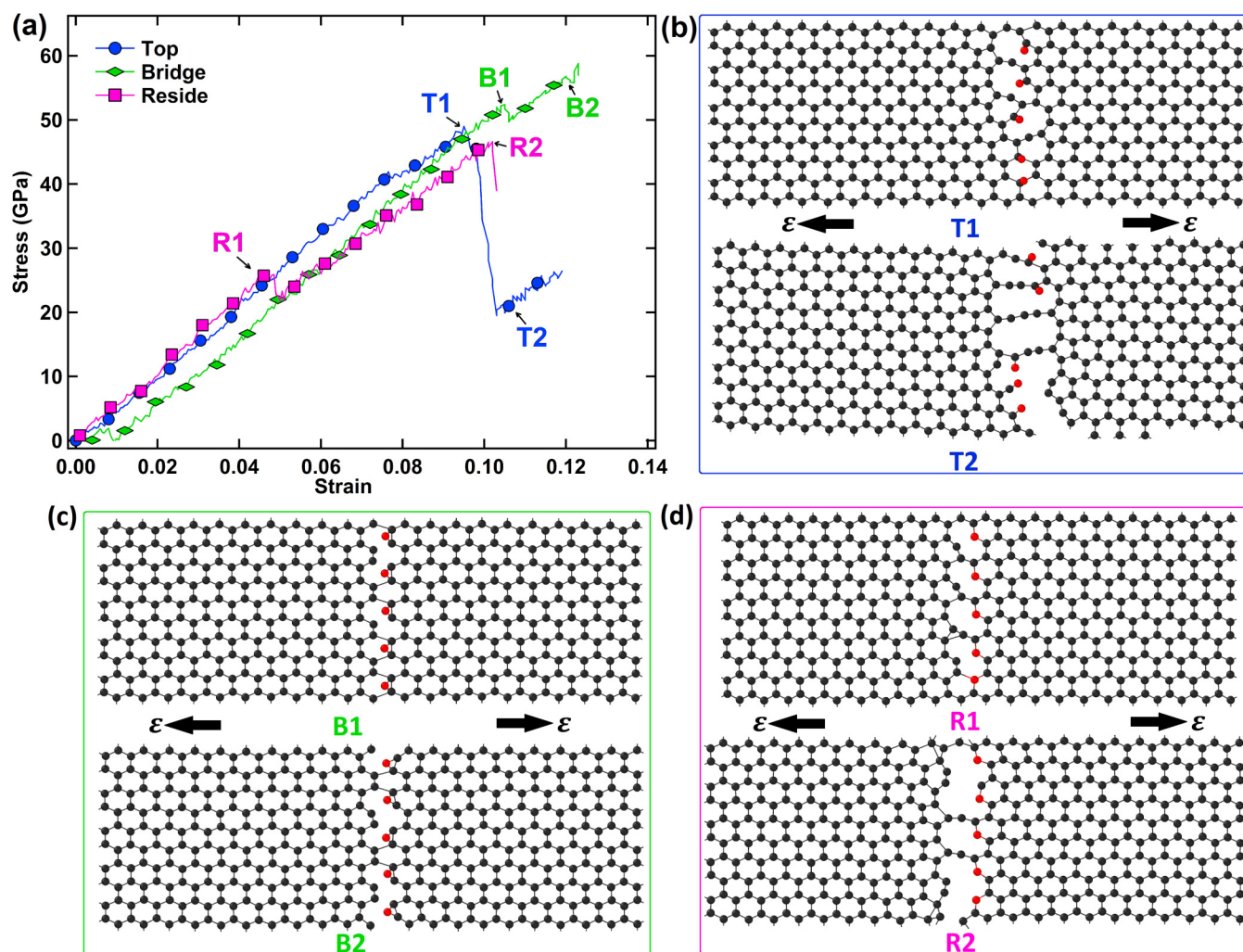


FIG. 3. (a) Tensile stress–strain curves of GO sheets with the top, bridge, and residue epoxide functional groups in a V-linear distribution and atomic configurations of GO sheets during the deformation of (b) top, (c) bridge, and (d) residue configurations, where each numbered group is represented in the stress–strain curves in panel (a). Oxygen and carbon atoms are indicated with red and gray colors, respectively.

Similar to V-linear, the stress changes linearly reaching the yield point, where post-peaks with plastic deformations can be observed upon further loading. Despite similar elastic behavior, the yield strength and post-peaks are dramatically different for epoxide configurations (Table I), which can be analyzed based on atomic deformations. The C–C bond break between the epoxide and sp^2 constitutes the yielding of the GO sheets with the top oxygen group [T1, Fig. 4(b)]. A crack propagation along sp^2 bonds is observed leading to post-peaks and cleavage [T2 and T3, Fig. 4(b)]. In contrast, at the yield point of GO sheets with the oxygen in the bridge configuration, epoxide functional groups transform into ether functional groups by breaking the C–C bonds associated with the epoxide ring [B1, Fig. 4(c)]. Crack nucleation and propagation are observed upon further deformations [B2 and B3, Fig. 4(c)]. The

deformation response of GO sheets with the random residue epoxide groups is nearly the same as those GO with the residue groups in the V-linear distribution shown in Fig. 3(d), where the C–O bond strength constitutes the yielding and post-peak behavior. Here, one random structure is considered to compare with the linear distributions, while the randomness of the epoxide configurations can slightly change the mechanical properties of GO.^{14,18}

Proceeding with monolayer GO with epoxide functional groups having a H-linear distribution, Fig. 5 demonstrates different mechanical behavior than the random and V-linear distributions (Figs. 3 and 4). The C–C bonds between sp^3 and sp^2 break at the yielding point of GO sheets with the top epoxide functional groups [T1, Fig. 5(b)]. Diagonal crack propagation is observed along with sp^2 carbon bonds upon more deformations [T2 and T3, Fig. 5(b)].

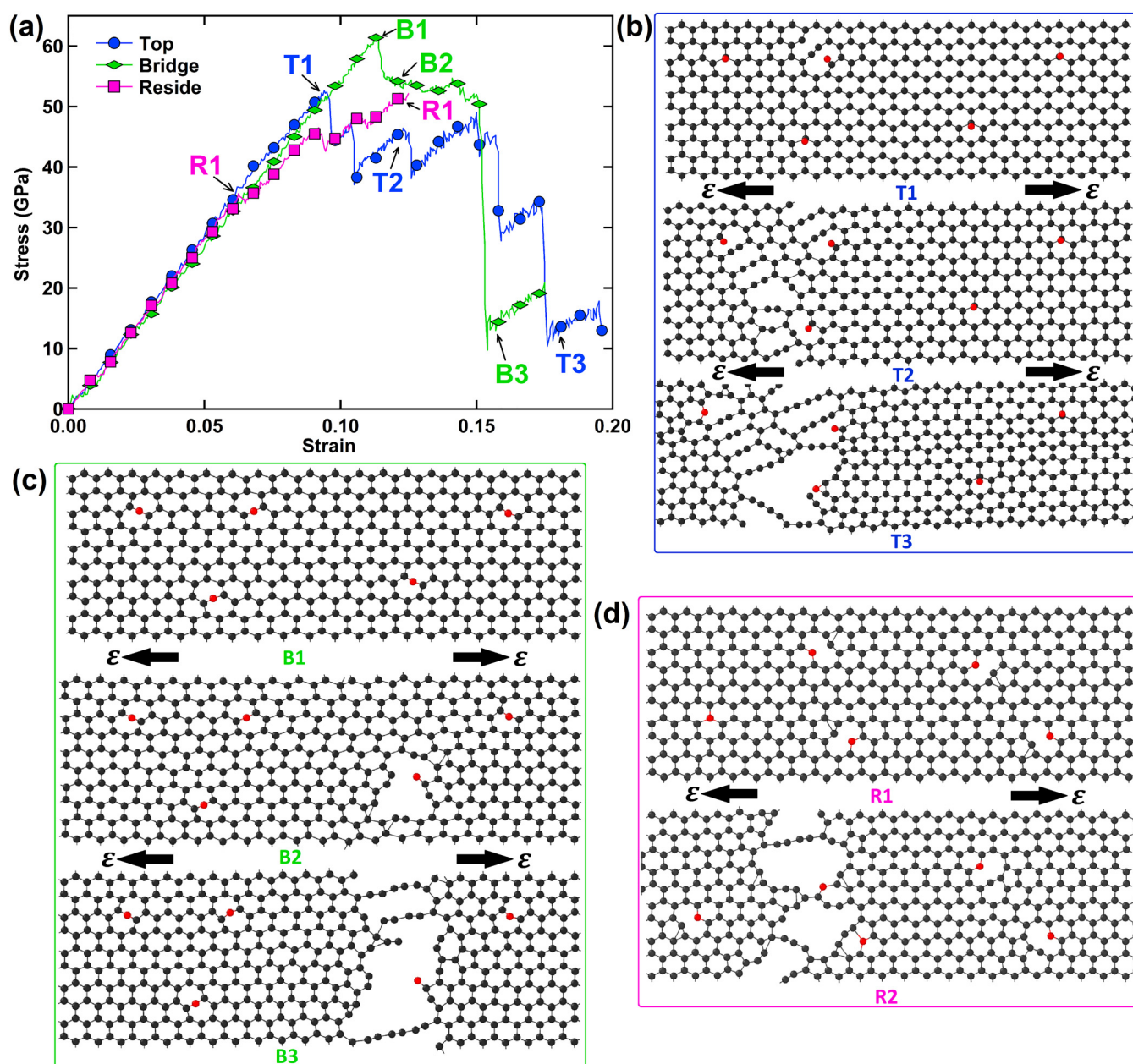


FIG. 4. (a) Tensile stress–strain curves of GO sheets with the top, bridge, and reside epoxide functional groups with a random distribution and atomic configurations of GO sheets during the deformation of (b) top, (c) bridge, and (d) reside configurations, where each numbered group is represented in the stress–strain curves in panel (a). Oxygen and carbon atoms are indicated with red and gray colors, respectively.

The bridge epoxide groups transform into ether groups leading to crack nucleation and yielding [B1, Fig. 5(c)]. Further deformation leads to a diagonal cleavage having an orientation of 45° with respect to the uniaxial load [B2 and B3 in Fig. 5(c)]. Although the C–O bond strength imposes a lower yield in the reside epoxide configuration compared to the top and bridge epoxide groups, the

post-peak deformation exhibits a similar crack propagation and cleavage [R2 and R3, Fig. 5(d)].

Results obtained in Table I exhibit a significant difference between the mechanical properties of pristine graphene and GO sheets, which can be linked to the transformation of sp^2 bonds in the pristine graphene into sp^3 bonds in GO.^{4,8,18} This change in the

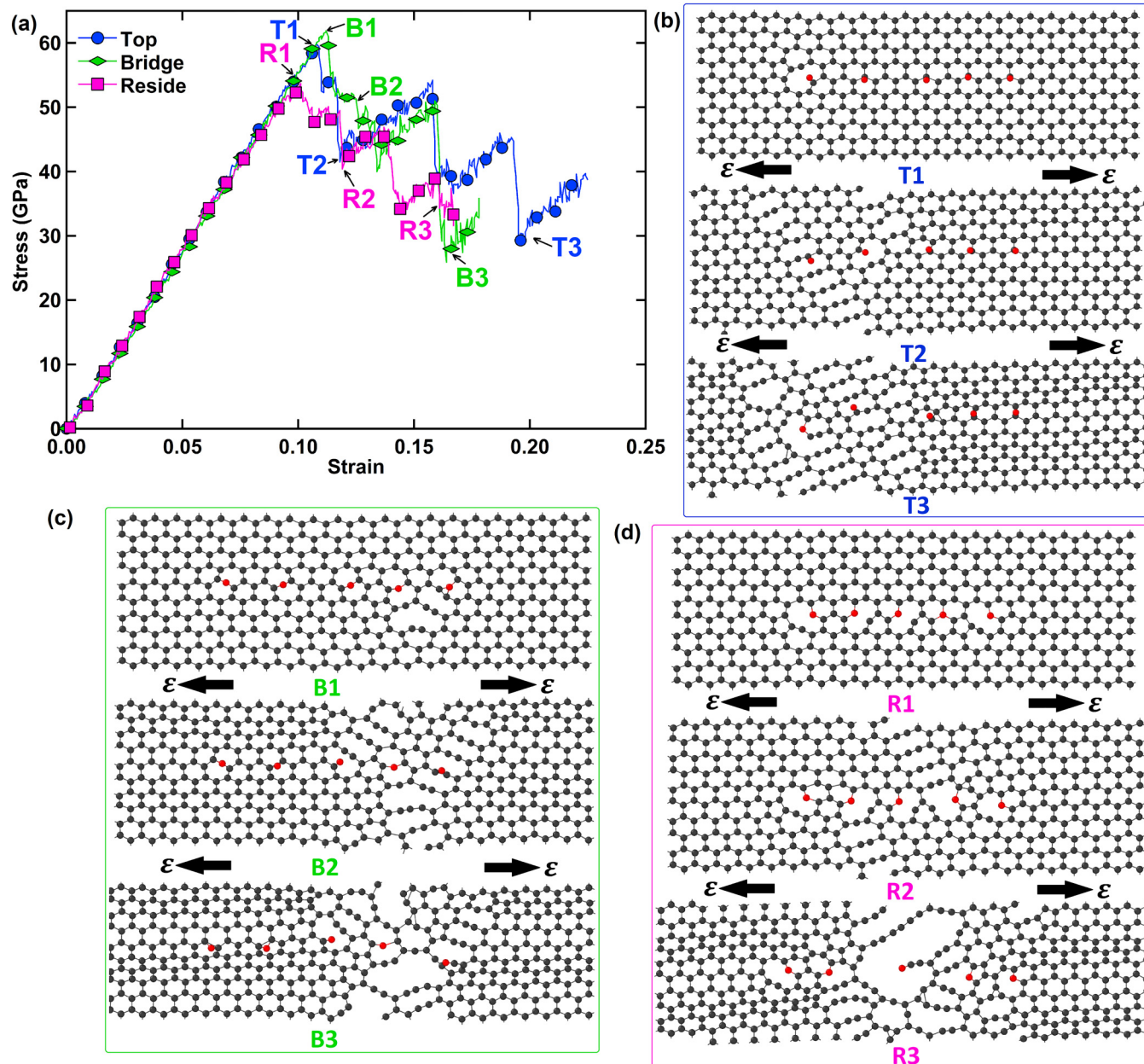


FIG. 5. (a) Tensile stress–strain curves of GO sheets with the top, bridge, and reside epoxide functional groups with a H-linear distribution and atomic configurations of GO sheets during the deformation of (b) top, (c) bridge, and (d) reside configurations, where each numbered group is represented in the stress–strain curves in panel (a). Oxygen and carbon atoms are indicated with red and gray colors, respectively.

bond structure can dramatically modify the mechanical behavior of GO. Any fluctuations in the elastic region can be linked to the thermal disturbances in the simulation box.^{13,18} A wide range of elastic modulus is reported previously for GO from 110 to 420 GPa, which is linked to the oxidation density and prestresses in GO sheets.^{6,9} This work demonstrates a change in the elastic

modulus from 480 to about 580 GPa due to the epoxide distribution and configuration, while the oxidation density remains the same. For the first time, the importance of an epoxide distribution and configuration on the mechanical behavior of GO sheets is studied. Results presented in Figs. 3–5 can be compared with previous theoretical works. For example, a similar fracture strain in GO

with the bridge epoxide group having a V-linear distribution is reported previously,¹⁹ while a higher fracture strength of about 97 GPa is estimated for GO. This difference can be linked to the considered thickness for monolayer GO. Some studies assume the pristine graphene thickness of 3.4 Å for GO,¹⁹ while a thickness of 7.5 Å is reported for monolayer GO.^{6,9} This has a significant effect on the estimated strength for GO. This work considers a thickness of 7.5 Å for monolayer GO. Therefore, a lower fracture strength predicted here (Table I) compared to some previous works¹⁹ can be linked to the assumed thickness for the monolayer GO. Overall, the elastic modulus and strength predicted in the present study are in the range of the mechanical properties of GO sheets with the same oxidation density reported previously.^{11,14,15,18,20} Although the ReaxFF potential has been used previously to model GO,^{11,13,14} the functional group density is the main focus to study the mechanical properties.^{15,18,20} This study reports the effect of various epoxide structures, for the first time, on the mechanical behavior of GO sheets.

The mechanical behavior of GO can be analyzed based on the epoxide configurations presented in Fig. 1. It was discussed previously that the C–C bonds between sp^3 and sp^2 constitute the strength of GO sheets with the top and bridge epoxide functional groups. In contrast, a weaker C–O bond imposes a lower strength for the reside functional group. In addition, regardless of distribution, a higher yield strength is obtained for the bridge epoxide group than the top configuration. This can be traced back to sp^3 carbon atoms and a bonding structure in the top and bridge epoxide groups. Starting from the top epoxide group [Fig. 1(a)], the sp^3 carbon atom moves out of the plane of sp^2 carbon atoms, which creates a diamond-like structure with rotated bonds between sp^3 and sp^2 carbon atoms.²⁷ This bond rotation forms two diamond-like structures in the bridge epoxide group [Fig. 1(b)], where two sp^3 carbon atoms jump out of the graphene plane.¹⁵ Previous works demonstrate a higher bonding distortion in the top configuration than the bridge one,¹⁵ which can be linked to the different tensile strengths of these epoxide groups.

Comparing the mechanical behavior of GO sheets in Figs. 3–5 exhibits the importance of epoxide configurations and their orientations. In contrast, the density of the epoxide group is another parameter controlling the mechanical properties of GO.^{14,18,20} The top and bridge configurations are reported to be common epoxide structures in GO sheets.¹⁹ After studying the effect of epoxide structures, the impact of top and bridge density on the mechanical behavior is studied, where the relative density, R , is considered

$$R = \frac{N_{C-SP3}}{N_C} \times 100, \quad (2)$$

where N_{C-SP3} and N_C are the number of sp^3 and total number of carbon atoms, respectively. The relative density, R , effect on the mechanical properties is evaluated for oxidation in a range of 1.2%–2.4% for a full top oxide to a full bridge epoxide, respectively. Figure 6 exhibits the change of the mechanical properties as a function of R . Results demonstrate a reduction in the elastic modulus from 580 to 525 GPa with changing R from 1.2% to 1.7%, while the elastic modulus remains the same for R more than 1.7%. In contrast, the yield strength changes from 52 to 61 GPa by increasing

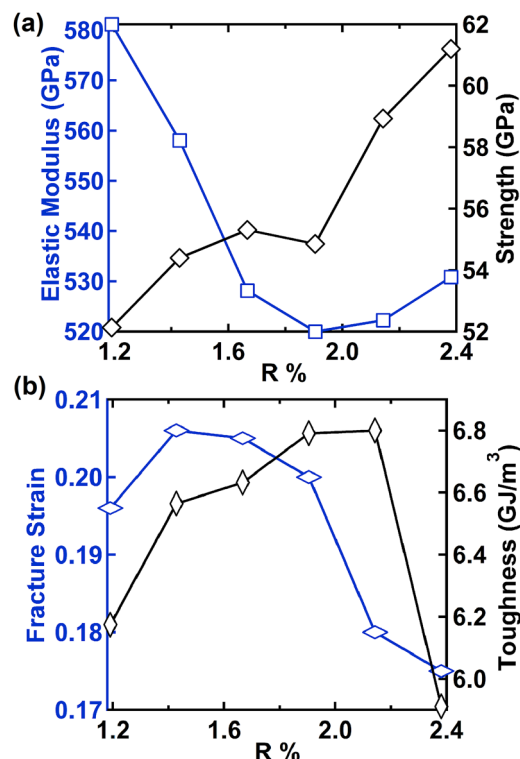


FIG. 6. The mechanical properties of GO as a function of R for (a) elastic modulus and yield strength and (b) fracture strain and toughness.

the bridge functional group. This change in the yield strength increases the fracture toughness for R less than 2.2%. The fracture toughness reduces considerably for R more than 2.2%, which can be linked to a dramatic decrease of the fracture strain for this relative density. The change of the fracture strain is found to be negligible for R less than 1.9%. Although the toughness of GO sheets fully decorated with the top and bridge configurations is similar, higher toughness is observed for GO sheets with a combination of both epoxide functional groups with R about 1.9%–2.2%. Previous studies report a reduction of the elastic modulus by increasing the oxidation density,^{14,20} where the ratio of epoxide-to-hydroxyl and oxidation levels is the main focus. Although it was demonstrated that the oxidation content and decreasing the number of epoxide-to-hydroxyl can reduce the strength and toughness,^{18,20} here, for the first time, it is presented that the mechanical properties of GO can be enhanced through increasing the relative density. This can be linked to the change of epoxide structures from the top configuration to the bridge configuration. In this respect, although the relative density increases in the bridge configuration compared to the top configuration, the mechanical properties is improved through changing the diamond-like structure of epoxide. Previous works report the importance of bonding transformation in the epoxide functional groups during the mechanical deformation of GO sheets.¹⁸

The influence of epoxide groups and their distribution on the mechanical behavior of GO is studied so far. The incorporation of electric fields and the mechanical behavior is an important aspect on the application of GO as electromechanical devices.^{28,29} Therefore, the interaction of electric fields on the epoxide functional groups is evaluated in the remainder. Figure 7 demonstrates the change of GO mechanical behavior in the electric field. Results show an insignificant effect of the electric field on the elastic properties and yield strength of GO sheets. The main impact of the electric field can be observed on the post-peak response in GO, with epoxide groups having the random and H-linear distributions [Figs. 7(b) and 7(c)]. For example, GO sheets with the bridge epoxide group randomly distributed under no electric field have a stress drop in a tensile strain of 0.15. At the same time, there is no stress drop after the yielding of those GO sheets under the electric field [Fig. 7(b)]. Although a broad post-peak region is observed in GO sheets with the randomly distributed residue group under the electric field, those GO sheets exhibit a brittle fracture without any electric field. The immediate impact of changing the post-peak behavior is the fracture toughness. Figure 7(d) shows the toughness properties of GO under the electric field. Results exhibit an insignificant electric field effect on the toughness of GO sheets with epoxide groups having the V-linear distribution. In contrast, the toughness under the electric field is significantly enhanced for GO sheets with the random epoxide group. Although the electric field reduces the toughness of the top and bridge epoxide groups with the H-linear distribution, the toughness under the electric field dramatically enhances for GO sheets with the residue configuration.

The impact of the electric field on the mechanical behavior of GO can be linked to the epoxide distortion. The electric field can change the binding energy followed by increasing the oxygen bond length in the diamond-like epoxide functional groups.^{24,32} Such an external in-plane force in GO nanoplatelets applies additional energy to the system. Therefore, higher strain energy is required to deform GO under the electric field compared to those without the electric field, leading to the toughness enhancement. Similar effects on the bonding energy have been observed in nanowires, where the change of surface energy has impacts on the mechanical properties of nanowires.³³ The presented study exhibits a benchmark study on the interaction of electric fields on the epoxide configurations, while understanding the effect of electric field modulation on the mechanical behavior of GO sheets necessitates further investigations. In addition to the electric field, there are various parameters having impacts on the mechanical response. For example, the effect of size is another important factor to be considered to model the mechanical behavior of nanostructures.^{34,35} Here, the impact of epoxide-rich regions is studied in GO sheets at the nanoscale, while scaling up this into the microscale with including all functional groups necessitates further investigations. The strain rate is another factor changing the mechanical behavior of materials. Although the strain rate has an insignificant effect on the mechanical properties of graphene,³⁶ GO deformation is strongly strain rate dependent.³⁷ This work exhibits the influence of oxidation on the mechanical properties of graphene, while defects can change the thermal behavior of graphene-based materials.³⁸ The structure of GO sheets can be a combination of various epoxide configurations with

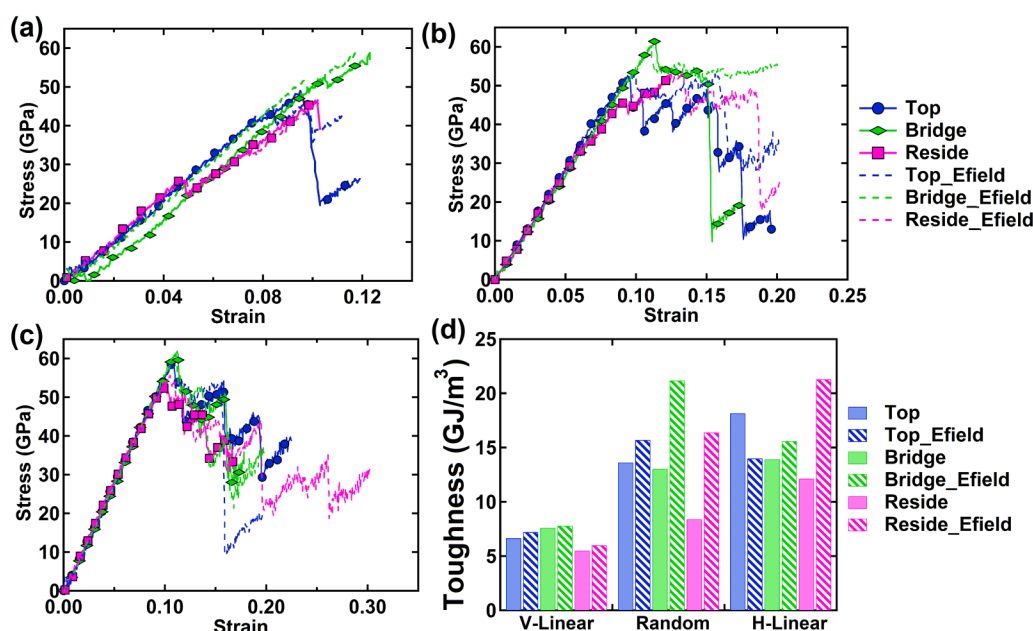


FIG. 7. Tensile stress-strain curves of GO sheets with an epoxide functional group having a (a) V-linear, (b) random, and (c) H-linear distribution along with the tensile load under an electric field (Efield) of 0.5 V/Å. (d) The toughness of GO sheets without and with an electric field.

different distributions,^{2,4} which can be fed into finite element approaches to model GO platelets.²¹

IV. CONCLUSION

This work uses the reactive MD simulations to study the effect of epoxide configurations on the mechanical properties of monolayer GO. Three epoxide structures are considered based on oxygen bonding with carbon atoms, including top, bridge, and reside structures, where those epoxide functional groups have linear and random distributions with respect to the applied load.

The major outcomes of this study are summarized as follows:

- A higher yield strength is observed in GO sheets with the bridge configuration compared to GO with the top and reside groups. In contrast, GO sheets with the reside functional group exhibit the lowest yield strength, regardless of the epoxide distribution.
- A brittle fracture is obtained for all epoxide configurations with the V-linear distribution, where the crack propagation occurs along the sp^3 bonds. GO sheets with the epoxide functional groups having the random and H-linear distributions demonstrate a ductile fracture.
- Epoxide configurations have a strong impact on the post-peak behavior and toughness of GO sheets. The highest toughness is obtained for GO with the top epoxide group having a H-linear distribution, while GO sheets with the reside configuration and the V-linear distribution show the lowest toughness.
- The change of the sp^3 bond density from 1.2% to 2.4% increases the yield strength from 52 to 61 GPa, while this change in the number of the sp^3 bond density reduces the fracture strain and elastic modulus.
- The external electric field can change the mechanical properties of GO, where the electric field enhances the mechanical toughness. This change is significant for GO sheets with the bridge and reside functional groups in the random and H-linear distributions, respectively.

Although previous works mainly focused on the degree of oxidation and concentration of functional groups, this study demonstrates the importance of epoxide configurations as well as their distributions on the mechanical properties of GO platelets. In addition to indicating new aspects to understand experimental observations, this work facilitates a guideline on potentials to control the mechanical properties of GO sheets through chemical compositions and using electric fields.

AUTHOR DECLARATIONS

Conflict of Interest

The authors have no conflicts to disclose.

Author Contributions

Mohammad Nasr Esfahani: Conceptualization (equal); Formal analysis (equal); Investigation (equal); Methodology (equal); Supervision (equal); Writing – original draft (equal); Writing – review & editing (equal). **Sepeede Shahbeigi:** Data curation (equal); Formal analysis (equal); Investigation (equal); Writing – review & editing (equal). **Masoud Jabbari:** Data curation (equal);

Investigation (equal); Project administration (equal); Writing – review & editing (equal).

DATA AVAILABILITY

The data that support the findings of this study are available from the corresponding author upon reasonable request.

REFERENCES

- ¹G. Eda and M. Chhowalla, “Chemically derived graphene oxide: Towards large-area thin-film electronics and optoelectronics,” *Adv. Mater.* **22**, 2392–2415 (2010).
- ²D. R. Dreyer, S. Park, C. W. Bielawski, and R. S. Ruoff, “The chemistry of graphene oxide,” *Chem. Soc. Rev.* **39**, 228–240 (2010).
- ³S.-J. Lee, S.-H. Jeong, D.-U. Kim, and J.-P. Won, “Effects of graphene oxide on pore structure and mechanical properties of cementitious composites,” *Compos. Struct.* **234**, 111709 (2020).
- ⁴Y. Zhu, S. Murali, W. Cai, X. Li, J. W. Suk, J. R. Potts, and R. S. Ruoff, “Graphene and graphene oxide: Synthesis, properties, and applications,” *Adv. Mater.* **22**, 3906–3924 (2010).
- ⁵C. Gómez-Navarro, M. Burghard, and K. Kern, “Elastic properties of chemically derived single graphene sheets,” *Nano Lett.* **8**, 2045–2049 (2008).
- ⁶J. W. Suk, R. D. Piner, J. An, and R. S. Ruoff, “Mechanical properties of monolayer graphene oxide,” *ACS Nano* **4**, 6557–6564 (2010).
- ⁷Y. Gao, L.-Q. Liu, S.-Z. Zu, K. Peng, D. Zhou, B.-H. Han, and Z. Zhang, “The effect of interlayer adhesion on the mechanical behaviors of macroscopic graphene oxide papers,” *ACS Nano* **5**, 2134–2141 (2011).
- ⁸S.-H. Kang, T.-H. Fang, Z.-H. Hong, and C.-H. Chuang, “Mechanical properties of free-standing graphene oxide,” *Diam. Relat. Mater.* **38**, 73–78 (2013).
- ⁹C. Cao, M. Daly, C. V. Singh, Y. Sun, and T. Filleter, “High strength measurement of monolayer graphene oxide,” *Carbon* **81**, 497–504 (2015).
- ¹⁰E. Gao, Y. Wen, Y. Yuan, C. Li, and Z. Xu, “Intrinsic mechanical properties of graphene oxide films: Strain characterization and the gripping effects,” *Carbon* **118**, 467–474 (2017).
- ¹¹D. Hou and T. Yang, “A reactive molecular dynamics study of graphene oxide sheets in different saturated states: Structure, reactivity and mechanical properties,” *Phys. Chem. Chem. Phys.* **20**, 11053–11066 (2018).
- ¹²N. V. Medhekar, A. Ramasubramaniam, R. S. Ruoff, and V. B. Shenoy, “Hydrogen bond networks in graphene oxide composite paper: Structure and mechanical properties,” *ACS Nano* **4**, 2300–2306 (2010).
- ¹³A. Verma and A. Parashar, “Molecular dynamics based simulations to study failure morphology of hydroxyl and epoxide functionalised graphene,” *Comput. Mater. Sci.* **143**, 15–26 (2018).
- ¹⁴X. Zhang, S. Liu, H. Liu, J. Zhang, and X. Yang, “Molecular dynamics simulation of the mechanical properties of multilayer graphene oxide nanosheets,” *RSC Adv.* **7**, 55005–55011 (2017).
- ¹⁵Y. Sun, X. Tang, H. Bao, Z. Yang, and F. Ma, “The effects of hydroxide and epoxide functional groups on the mechanical properties of graphene oxide and its failure mechanism by molecular dynamics simulations,” *RSC Adv.* **10**, 29610–29617 (2020).
- ¹⁶M. Tavakol, A. Montazeri, S. H. Aboutalebi, and R. Asgari, “Mechanical properties of graphene oxide: The impact of functional groups,” *Appl. Surf. Sci.* **525**, 146554 (2020).
- ¹⁷Y. Sun, L. Chen, L. Cui, Y. Zhang, and X. Du, “Molecular dynamics simulation of the effect of oxygen-containing functional groups on the thermal conductivity of reduced graphene oxide,” *Comput. Mater. Sci.* **148**, 176–183 (2018).
- ¹⁸R. A. Soler-Crespo, W. Gao, P. Xiao, X. Wei, J. T. Paci, G. Henkelman, and H. D. Espinosa, “Engineering the mechanical properties of monolayer graphene oxide at the atomic level,” *J. Phys. Chem. Lett.* **7**, 2702–2707 (2016).
- ¹⁹J. T. Paci, T. Belytschko, and G. C. Schatz, “Computational studies of the structure, behavior upon heating, and mechanical properties of graphite oxide,” *J. Phys. Chem. C* **111**, 18099–18111 (2007).

- ²⁰L. Liu, J. Zhang, J. Zhao, and F. Liu, "Mechanical properties of graphene oxides," *Nanoscale* **4**, 5910–5916 (2012).
- ²¹I. Benedetti, H. Nguyen, R. A. Soler-Crespo, W. Gao, L. Mao, A. Ghasemi, J. Wen, S. Nguyen, and H. D. Espinosa, "Formulation and validation of a reduced order model of 2D materials exhibiting a two-phase microstructure as applied to graphene oxide," *J. Mech. Phys. Solids* **112**, 66–88 (2018).
- ²²Z. Liu, K. Nørgaard, M. H. Overgaard, M. Ceccato, D. M. Mackenzie, N. Stenger, S. L. Stipp, and T. Hassenkam, "Direct observation of oxygen configuration on individual graphene oxide sheets," *Carbon* **127**, 141–148 (2018).
- ²³K. Erickson, R. Erni, Z. Lee, N. Alem, W. Gannett, and A. Zettl, "Determination of the local chemical structure of graphene oxide and reduced graphene oxide," *Adv. Mater.* **22**, 4467–4472 (2010).
- ²⁴H. L. Mai, X.-Y. Cui, C. Stampfl, and S. P. Ringer, "The role of vacancies in electric field mediated graphene oxide reduction," *Appl. Phys. Lett.* **113**, 073103 (2018).
- ²⁵S. Plimpton, "Fast parallel algorithms for short-range molecular dynamics," *J. Comput. Phys.* **117**, 1–19 (1995).
- ²⁶K. Chenoweth, A. C. Van Duin, and W. A. Goddard, "ReaxFF reactive force field for molecular dynamics simulations of hydrocarbon oxidation," *J. Phys. Chem. A* **112**, 1040–1053 (2008).
- ²⁷Q. Pei, Y. Zhang, and V. Shenoy, "A molecular dynamics study of the mechanical properties of hydrogen functionalized graphene," *Carbon* **48**, 898–904 (2010).
- ²⁸T. Q. Trung, N. T. Tien, D. Kim, M. Jang, O. J. Yoon, and N.-E. Lee, "A flexible reduced graphene oxide field-effect transistor for ultrasensitive strain sensing," *Adv. Funct. Mater.* **24**, 117–124 (2014).
- ²⁹Z. Chang, J. Deng, G. G. Chandrakumara, W. Yan, and J. Z. Liu, "Two-dimensional shape memory graphene oxide," *Nat. Commun.* **7**, 11972 (2016).
- ³⁰C. Guo, Y. Cai, H. Zhao, D. Wang, Y. Hou, J. Lv, H. Qu, D. Dai, X. Cai, J. Lu, and J. Cai, "Efficient synthesis of graphene oxide by Hummers method assisted with an electric field," *Mater. Res. Express* **6**, 055602 (2019).
- ³¹J. Y. Kim and S. O. Kim, "Electric fields line up graphene oxide," *Nat. Mater.* **13**, 325–326 (2014).
- ³²M. Topsakal, H. H. Gurel, and S. Ciraci, "Effects of charging and electric field on graphene oxide," *J. Phys. Chem. C* **117**, 5943–5952 (2013).
- ³³J. Zhang and C. Wang, "Effect of the electric field on the mechanical properties of gallium nitride nanowires," *Europhys. Lett.* **105**, 28004 (2014).
- ³⁴M. Nasr Esfahani and B. E. Alaca, "A review on size-dependent mechanical properties of nanowires," *Adv. Eng. Mater.* **21**, 1900192 (2019).
- ³⁵H. Bu, Y. Chen, M. Zou, H. Yi, K. Bi, and Z. Ni, "Atomistic simulations of mechanical properties of graphene nanoribbons," *Phys. Lett. A* **373**, 3359–3362 (2009).
- ³⁶H. Zhao and N. Aluru, "Temperature and strain-rate dependent fracture strength of graphene," *J. Appl. Phys.* **108**, 064321 (2010).
- ³⁷S. Vinod, C. S. Tiwary, L. D. Machado, S. Ozden, J. Cho, P. Shaw, R. Vajtai, D. S. Galvão, and P. M. Ajayan, "Strain rate dependent shear plasticity in graphite oxide," *Nano Lett.* **16**, 1127–1131 (2016).
- ³⁸M. N. Esfahani, M. Jabbari, Y. Xu, and C. Soutis, "Effect of nanoscale defects on the thermal conductivity of graphene," *Mater. Today Commun.* **26**, 101856 (2021).